# Whole genome CRISPR screening identifies TOP2B as a potential target for IMiD sensitization in multiple myeloma

*Matteo Costacurta,[1,2] Stephin J Vervoort,[1,2] Simon J Hogg,[1,2] Benjamin P Martin,[1,2] Ricky W Johnstone[1,2#] and Jake Shortt[1,2,3,4#]*

*[1]Translational Hematology Program, Peter MacCallum Cancer Center, Melbourne; [2]Peter MacCallum Department of Oncology, The University of Melbourne, Parkville, Melbourne; [3]Monash Hematology, Monash Health, Clayton, Melbourne and [4]Blood Cancer Therapeutics Laboratory, School of Clinical Sciences at Monash Health, Monash University, Clayton, Melbourne, Victoria, Australia.*

*[#]RWJ and JS contrituted equally as co-senior authors.*

*Correspondence: RICKY W. JOHNSTONE - ricky.johnstone@petermac.org*
*JAKE SHORTT - jake.shortt@monash.edu*

*doi:10.3324/haematol.2020.265611*

**Supplementary Figures**

**Figure S1. GO and PPI analysis of genome-wide CRISPR resistance KO screen**

(A) Normalized read counts (in log2) at the end of the screen of sgRNAs specific for *IRF4*, *MYC*, *IKZF1* and *IKZF3* in DMSO-treated MM.1S-Cas9 cells at the end of the screen. The average counts in DMSO T-End are compared to the T-0 reference, respectively. (A) PPI network of MM.1S-Cas9 cells unique dependencies (metascape). (B) GO analysis of MM.1S unique dependencies. (C) PPI network of MM.1S-Cas9 cells unique dependencies (metascape). (D) Venn diagram of overlapping hits between our CRISPR resistance screen and those of Sievers et al. and Liu et al[5,6]. (E) Normalized read counts (in log2) at the end of the screen of sgRNAs targeting CRBN in MM.1S-Cas9 cells in the LEN and POM conditions. The average counts in LEN and POM T-End are compared to the DMSO T-End condition, respectively. (F) PPI network of hits in MM.1S-Cas9 cells treated with LEN at the end of the resistance screen (STRING). (G) GO analysis of hits in MM.1S-Cas9 cells treated with LEN at the end of the resistance screen (ToppFun). FDR values are represented as -log10.

**Figure S2. GO and PPI analysis of MM.1S and MM.1Sres dependencies**

(A) PPI network of MM.1Sres-Cas9 cells unique dependencies (metascape). (B) GO analysis of MM.1Sres-Cas9 cells unique dependencies. (C) Venn diagram of MM.1S-Cas9 and MM.1Sres-Cas9 cells dependencies (adjusted $P < 0.05$). (D) GO analysis of MM.1S-Cas9 and MM.1Sres-Cas9 cells mutual dependencies. (E) Scatter plot representing the log2 fold change of sgRNAs (dependencies) that are significant for adjusted $P < 0.05$. The regression line represents Pearson's correlation with relative Pearson's coefficient value R and the level of significance p. (F) Normalized read counts (in log2) at the end of the screen of sgRNAs specific for *IRF4*, *MYC*, *IKZF1* and *IKZF3* in DMSO-treated MM.1Sres-Cas9 cells at the end of the screen. The average counts in DMSO T-End are compared to the T-0 reference, respectively. (G) Immunoblot validating CRISPR-mediated *TOP2B* KO in MM.1S and MM.1Sres cells expressing Cas9. Actin is provided as loading control.

**Figure S3. Impact of genetic TOP2B deletion or TOP2 inhibition on the expression of CRBN, the IKZF1/3-IRF4-MYC axis and the cell cycle, upon IMiD treatment**

(A) Immunoblot showing expression of TOP2B and CRBN in MM.1S-Cas9 and MM.1Sres Cas9 TOP2B KO cells relative to their controls (MM.1S-Cas9 and MM.1Sres Cas9 SCR BFP and SCR GFP cells). Actin is provided as loading control. (B) Western blot displaying degradation of IKZF3 in MM.1Sres-Cas9 TOP2B KO cells in comparison to MM.1Sres SCR GFP cells after 16h of treatment with DMSO, 2μM LEN or 500nM POM. Actin is provided as loading control. (C) Immunoblot showing expression of IRF4 and MYC in MM.1Sres-Cas9 TOP2B KO cells in comparison to MM.1Sres SCR GFP cells after 72h of treatment with DMSO, 2μM LEN or 500nM POM. HSP90 is provided as loading control. (D) FACS histogram plots of $PI^+$ cells showing the effect on MM.1S and MM.1Sres cells of DMSO, LEN, DXZ and the combination treatment (histograms are representative of one of three independent experiment). (E) and (F) Bar plots showing proportion of Nicoletti-stained MM.1S and MM.1Sres cells, respectively, in SubG1, S-Phase and >2N (DNA content higher than that in G2M) as aggregate of three independent biological replicates with three technical replicates each. Error bars represent mean ± standard error of the mean of three independent experiments. v=significant vs vehicle (DMSO), l=significant vs LEN, d=significant vs DXZ ($P < 0.05$). (G) Immunoblot showing expression of TOP2B, IKZF3 and CRBN in MM.1S and MM.1Sres cells treated for 16 hours with DMSO, LEN (2μM), DXZ (20μM) or combined treatment for 16 hours. Actin is provided as loading control. (H) Immunoblot displaying expression of gamma-H2AX as marker of DNA damage in MM.1S and MM.1Sres cells treated with DMSO, LEN (2μM), etoposide (10μM) or combo for 16 hours. Tubulin is provided as loading control. (I) Bar plot representing percentage of viable cells (PI negative, by FACS analysis) of MM.1S and MM.1Sres exposed to prolonged treatment (7 days) with DMSO, LEN (2μM), etoposide (312nM) and Combo. Error bars represent mean ± standard error of the mean of three independent experiments with two technical replicates each. v=significant vs vehicle (DMSO), l=significant vs LEN, e=significant vs etoposide ($P < 0.05$). (J) Dependency score (extracted from the DepMap repository) of the genes *TOP2A* and *TOP2B* in MM cell lines (MM) and other tumours (Non-MM). A value of 0 represents a non-dependency, a value of -1 or below represents a dependency.

# Figure S1

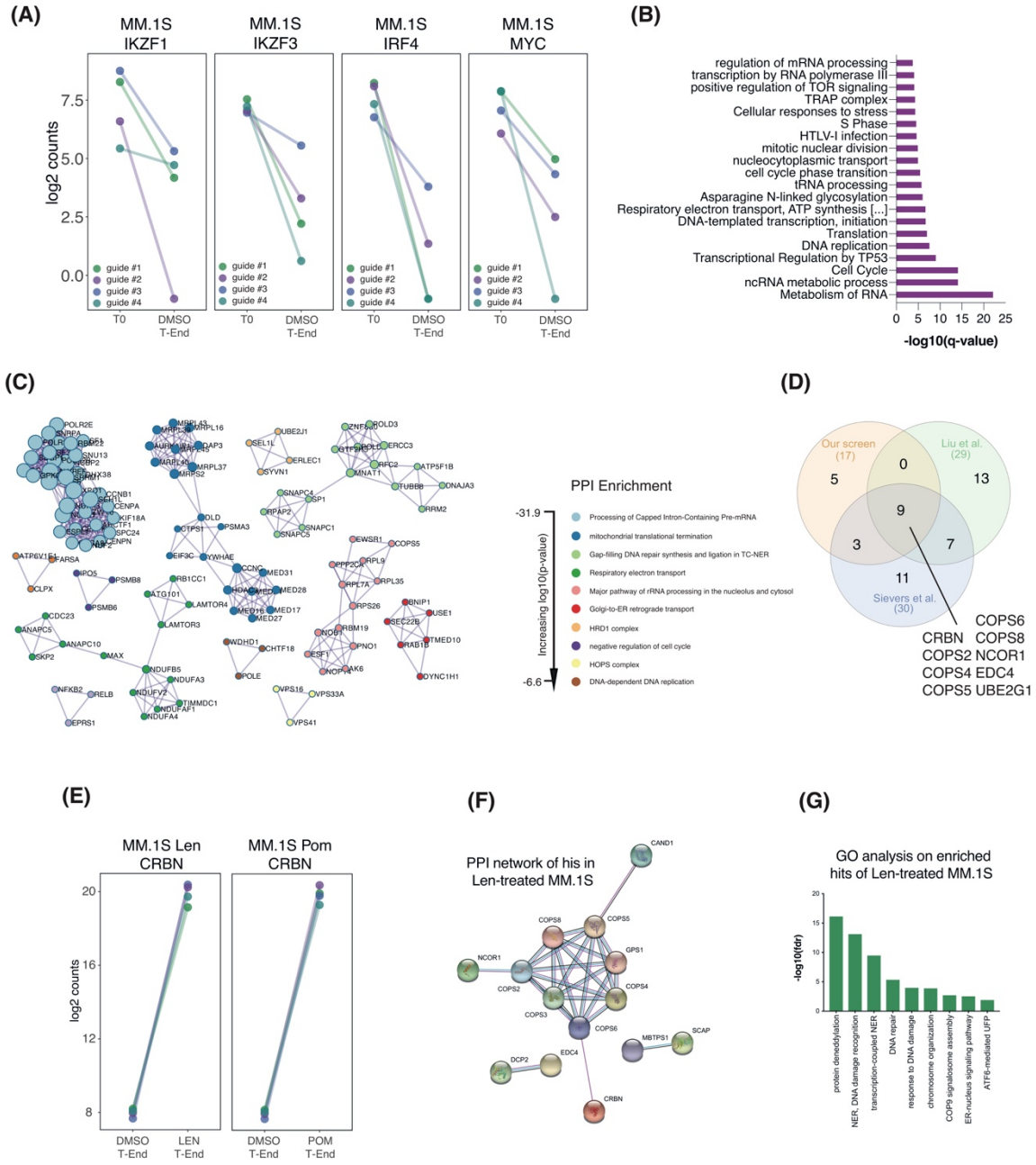
(A)
MM.1S IKZF1
MM.1S IKZF3
MM.1S IRF4
MM.1S MYC
log2 counts
7.5
5.0
2.5
0.0
guide #1
guide #2
guide #3
guide #4
T0
DMSO T-End
(B)
regulation of mRNA processing
transcription by RNA polymerase III
positive regulation of TOR signaling
TRAP complex
Cellular responses to stress
S Phase
HTLV-I infection
mitotic nuclear division
nucleocytoplasmic transport
cell cycle phase transition
tRNA processing
Asparagine N-linked glycosylation
Respiratory electron transport, ATP synthesis [...]
DNA-templated transcription, initiation
Translation
DNA replication
Transcriptional Regulation by TP53
Cell Cycle
ncRNA metabolic process
Metabolism of RNA
0 5 10 15 20 25
-log10(q-value)
(C)
PPI Enrichment
-31.9
-6.6
Increasing log10(p-value)
Processing of Capped Intron-Containing Pre-mRNA
mitochondrial translational termination
Gap-filling DNA repair synthesis and ligation in TC-NER
Respiratory electron transport
Major pathway of rRNA processing in the nucleolus and cytosol
Golgi-to-ER retrograde transport
HRD1 complex
negative regulation of cell cycle
HOPS complex
DNA-dependent DNA replication
(D)
Our screen (17)
Liu et al. (29)
Sievers et al. (30)
5
0
13
9
3
7
11
CRBN
COPS6
COPS8
COPS2
NCOR1
COPS4
EDC4
COPS5
UBE2G1
(E)
MM.1S Len CRBN
MM.1S Pom CRBN
log2 counts
20
16
12
8
DMSO T-End
LEN T-End
DMSO T-End
POM T-End
(F)
PPI network of his in Len-treated MM.1S
CAND1
COPS8
COPS5
GPS1
NCOR1
COPS2
COPS4
COPS3
COPS6
MBTPS1
SCAP
DCP2
EDC4
CRBN
(G)
GO analysis on enriched hits of Len-treated MM.1S
-log10(fdr)
20
15
10
5
0
protein deneddylation
NER, DNA damage recognition
transcription-coupled NER
DNA repair
response to DNA damage
chromosome organization
COP9 signalosome assembly
ER-nucleus signaling pathway
ATF6-mediated UPR

# Figure S2

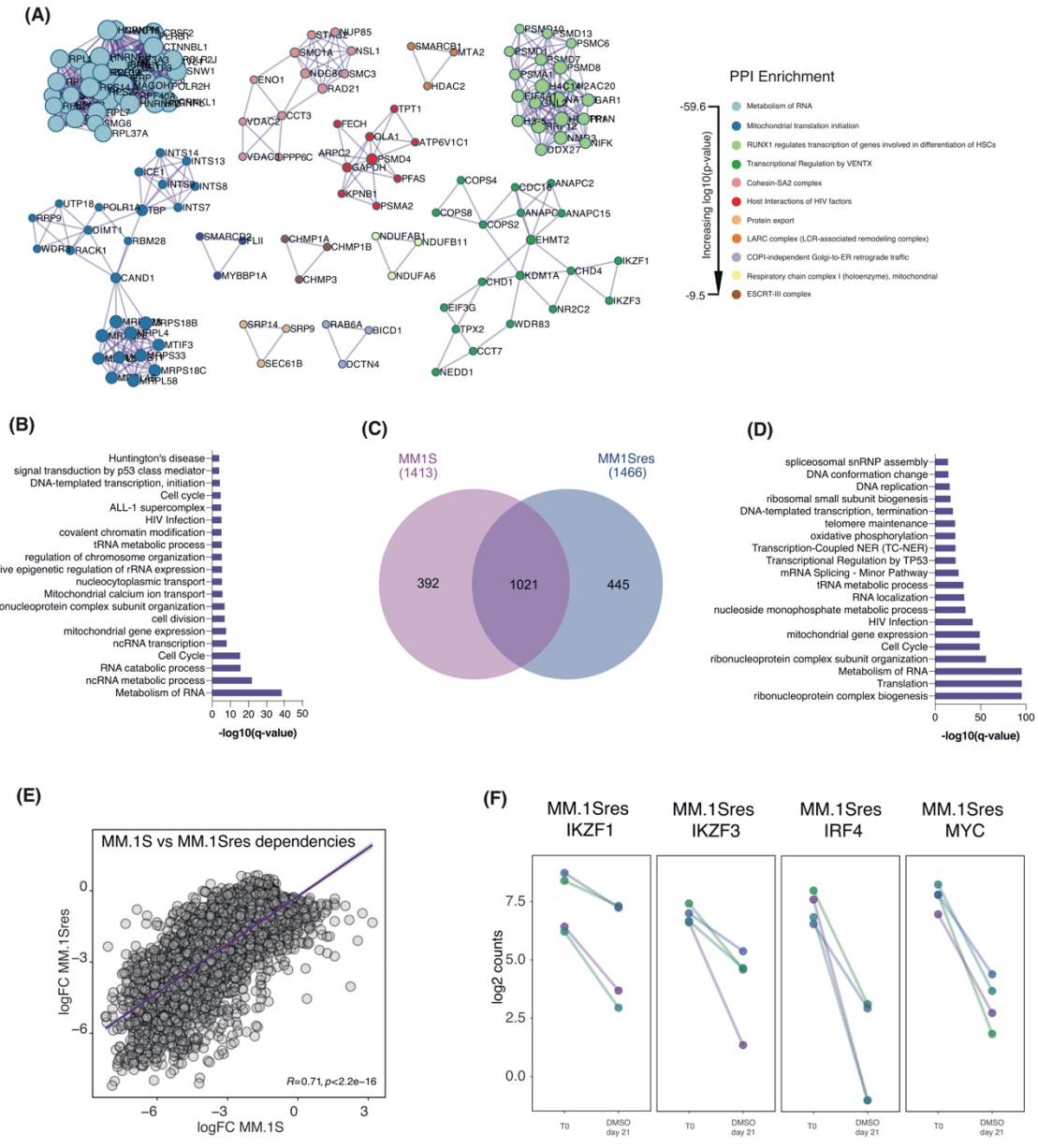
(A)
PPI Enrichment
-59.6
-9.5
Increasing log10(p-value)
Metabolism of RNA
Mitochondrial translation initiation
RUNX1 regulates transcription of genes involved in differentiation of HSCs
Transcriptional Regulation by VENTX
Cohesin-SA2 complex
Host Interactions of HIV factors
Protein export
LARC complex (LCR-associated remodeling complex)
COPI-independent Golgi-to-ER retrograde traffic
Respiratory chain complex I (holoenzyme), mitochondrial
ESCRT-III complex
(B)
Huntington's disease
signal transduction by p53 class mediator
DNA-templated transcription, initiation
Cell cycle
ALL-1 supercomplex
HIV Infection
covalent chromatin modification
tRNA metabolic process
regulation of chromosome organization
Positive epigenetic regulation of rRNA expression
nucleocytoplasmic transport
Mitochondrial calcium ion transport
ribonucleoprotein complex subunit organization
cell division
mitochondrial gene expression
ncRNA transcription
Cell Cycle
RNA catabolic process
ncRNA metabolic process
Metabolism of RNA
0 10 20 30 40 50
-log10(q-value)
(C)
MM1S
(1413)
MM1Sres
(1466)
392
1021
445
(D)
spliceosomal snRNP assembly
DNA conformation change
DNA replication
ribosomal small subunit biogenesis
DNA-templated transcription, termination
telomere maintenance
oxidative phosphorylation
Transcription-Coupled NER (TC-NER)
Transcriptional Regulation by TP53
mRNA Splicing - Minor Pathway
tRNA metabolic process
RNA localization
nucleoside monophosphate metabolic process
HIV Infection
mitochondrial gene expression
Cell Cycle
ribonucleoprotein complex subunit organization
Metabolism of RNA
Translation
ribonucleoprotein complex biogenesis
0 50 100
-log10(q-value)
(E)
MM.1S vs MM.1Sres dependencies
logFC MM.1Sres
logFC MM.1S
R=0.71, p<2.2e-16
(F)
MM.1Sres IKZF1
MM.1Sres IKZF3
MM.1Sres IRF4
MM.1Sres MYC
log2 counts
T0
DMSO day 21

# Figure S3

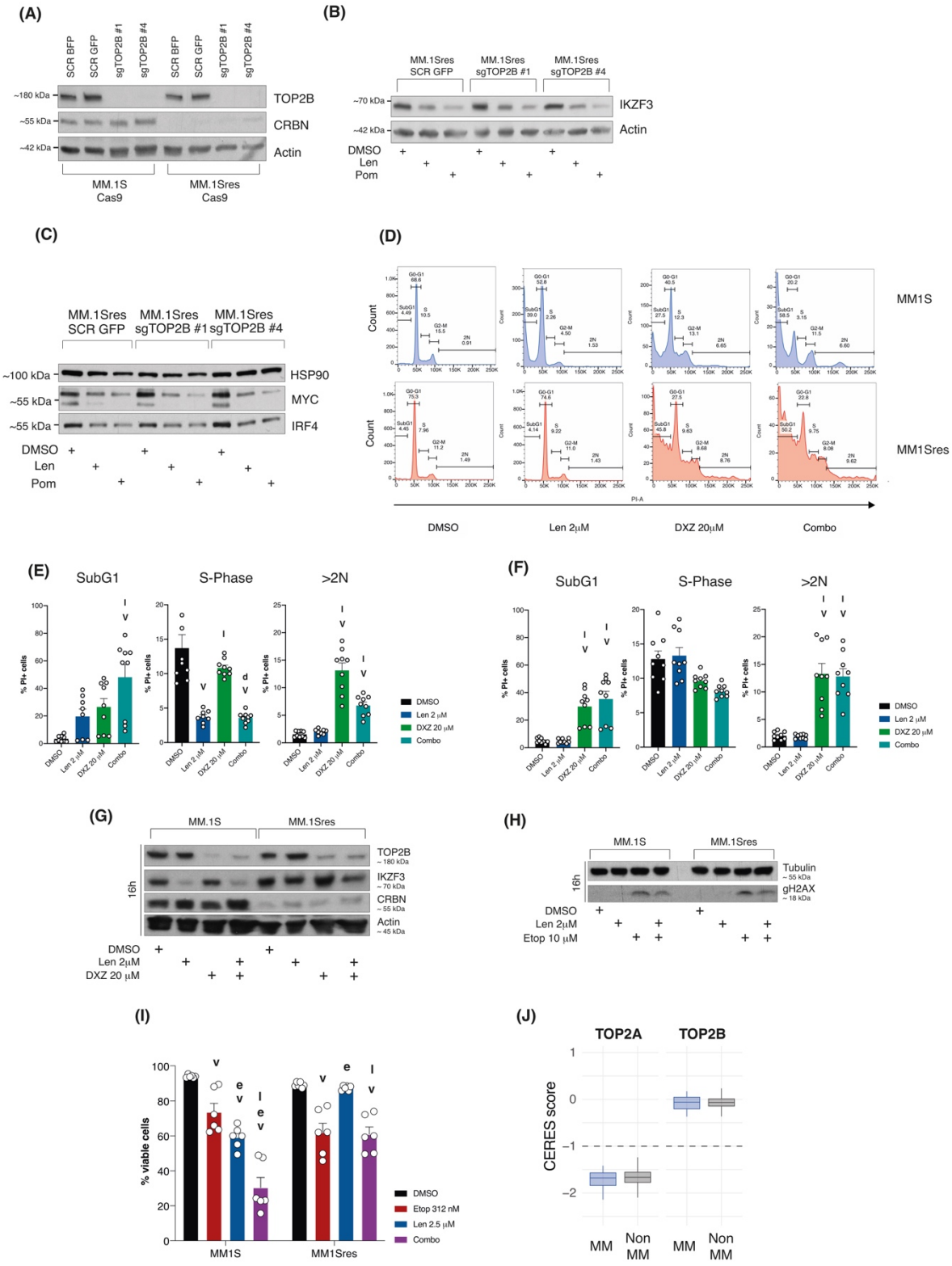
(A)
SCR BFP
SCR GFP
sgTOP2B #1
sgTOP2B #4
~180 kDa
~55 kDa
~42 kDa
TOP2B
CRBN
Actin
MM.1S Cas9
MM.1Sres Cas9
(B)
MM.1Sres SCR GFP
MM.1Sres sgTOP2B #1
MM.1Sres sgTOP2B #4
~70 kDa
~42 kDa
IKZF3
Actin
DMSO
Len
Pom
(C)
MM.1Sres SCR GFP
MM.1Sres sgTOP2B #1
MM.1Sres sgTOP2B #4
~100 kDa
~55 kDa
~55 kDa
HSP90
MYC
IRF4
DMSO
Len
Pom
(D)
Count
MM1S
MM1Sres
PI-A
DMSO
Len 2μM
DXZ 20μM
Combo
(E)
SubG1
S-Phase
>2N
% PI+ cells
DMSO
Len 2 μM
DXZ 20 μM
Combo
(F)
SubG1
S-Phase
>2N
% PI+ cells
DMSO
Len 2 μM
DXZ 20 μM
Combo
(G)
MM.1S
MM.1Sres
16h
TOP2B
~180 kDa
IKZF3
~70 kDa
CRBN
~55 kDa
Actin
~45 kDa
DMSO
Len 2μM
DXZ 20 μM
(H)
MM.1S
MM.1Sres
16h
Tubulin
~55 kDa
gH2AX
~18 kDa
DMSO
Len 2μM
Etop 10 μM
(I)
% viable cells
DMSO
Etop 312 nM
Len 2.5 μM
Combo
MM1S
MM1Sres
(J)
TOP2A
TOP2B
CERES score
MM
Non MM
MM
Non MM